Triboson Excesses in light of a Real Higgs Triplet Model

Srimoy Bhattacharya[1,2], **Siddharth P. Maharathy**[1,2,3], **Mukesh Kumar** [1], **Andreas Crivellin**[4], **Yaquan Fang** [5], **Rachid Mazini** [1], **and Bruce Mellado**[1,2]

[1]School of Physics and Institute for Collider Particle Physics, University of the Witwatersrand, Johannesburg, South Africa
[2]iThemba LABS, National Research Foundation, PO Box 722, Somerset West 7129, South Africa
[3]Indian Institute of Science Education and Research Pune, Dr. Homi Bhabha Road, Pune 411008, India
[4]Physik-Institut, Universität Zürich, Winterthurerstrasse 190, CH–8057 Zürich, Switzerland
[5]Institute of High Energy Physics ,19B, Yuquan Road, Shijing District, 100049, Beijing,China

E-mail: srimoy.bhattacharya@wits.ac.za

Abstract. Recent multilepton anomalies, which are defined as persistent excesses in final states with multiple leptons, missing energy, and (b-)jets, suggest the presence of a new scalar beyond the Standard Model (SM). Excesses in higgs to diphoton, $Z\gamma$, and WW spectra hint at a Higgs-like scalar S with mass $m_S \approx 152 \pm 1$ GeV, while the ZZ channel remains SM-like. This signature can be explained with a Real Higgs Triplet (RHT) model with hypercharge $Y = 0$, where S does not couple to ZZ at tree level. The Triplet scalars with mass m_s can be produced via Drell–Yan process and decay to electroweak bosons, enhancing triboson final states such as WWZ, WZZ, and WWW. Intriguingly, both ATLAS and CMS have reported significant excesses in such triboson channels, with observed (expected) significances reaching 6.4σ (4.7σ) in the VVZ (where $V = W$ or Z) channel and 4.4σ (3.6σ) in WWZ, raising the possibility that these signals may be the manifestations of an extended Higgs sector. We investigate whether the RHT model can account for these triboson excesses through electroweak production and decay of triplet scalars.

1 Introduction

The discovery of the Higgs boson in 2012 confirmed the completeness of the Standard Model (SM). However, experimental results from various LHC experiments have increasingly pointed toward the possibility of physics beyond the SM (BSM). Among the most compelling hints are the so-called "multilepton anomalies" - statistically significant deviations in channels featuring multiple leptons, missing energy, and possibly (b-)jets in the final state - compared to SM predictions. These anomalies suggest the production of BSM scalar particles at the electroweak scale, possibly in association with SM particles.

A particularly compelling scenario involves the production of a heavier scalar resonance, which primarily decays into a pair of lighter scalars, S, with mass $\approx 150 \pm 5$ GeV. This cascade decay naturally gives rise to final states rich in electroweak bosons and leptons, offering a coherent explanation for the multilepton excesses observed in LHC data. In Refs. [1, 2], the sidebands of SM Higgs searches by ATLAS and CMS [3–10] have been analyzed, concluding that the observed data favor a narrow scalar resonance with a mass of approximately 152 GeV in the diphoton and $Z\gamma$ invariant mass spectra, with a global significance exceeding 5σ. However, no excess is seen in the ZZ channel. This pattern disfavors simple Higgs doublet extensions but aligns naturally with

Center of Mass Energy	Process	Observed Cross section (fb)	Expected Cross section (fb)
$\sqrt{s} = 13$ TeV	WWZ	$442 \pm 94(\text{stat.})^{+60}_{-52}(\text{syst.})$ [11]	329.0 [11]
		$300^{+120}_{-100}(\text{stat.})^{+50}_{-40}(\text{syst.})$ [12]	354.0 [12]
		$280^{+120}_{-110}(\text{stat.})^{+40}_{-30}(\text{syst.})$ [13]	373.0 [13]
	WZZ	$200^{+111}_{-91}(\text{stat.})^{+65}_{-37}(\text{syst.})$ [11]	93.1 [11]
		$200^{+160}_{-110}(\text{stat.})^{+70}_{-20}(\text{syst.})$ [12]	91.6 [12]
	WWW	$820 \pm 100(\text{stat.}) \pm 80(\text{syst.})$ [14]	511.0 ± 18 [14]
	tWZ	$248 \pm 38(\text{stat.}) \pm 35(\text{syst.})$ [15]	136.0^{+9}_{-8} [15]
$\sqrt{s} = 13.6$ TeV	WWZ	$700^{+270}_{-230}(\text{stat})^{+90}_{-60}(\text{syst})$ [13]	402 [13]
	tWZ	$242 \pm 62(\text{stat.}) \pm 46(\text{syst.})$ [15]	147.8^{+10}_{-9} [15]

Table 1: Observed and expected inclusive cross sections for WWZ, WZZ, WWW and tWZ production.

a Real Higgs Triplet (RHT) model with hypercharge $Y = 0$, where the new scalar S does not couple to ZZ at tree level. The RHT model also predicts triboson signatures - WWW, WWZ, WZZ - from pair-produced triplet scalars decaying into electroweak bosons. Intriguingly, both ATLAS and CMS have also observed excesses in these channels.

Table 1 summarizes recent ATLAS and CMS measurements of inclusive cross sections for WWZ, WZZ, WWW, and tWZ production at $\sqrt{s} = 13$ and 13.6 TeV, compared with SM predictions at NLO in QCD. Several channels exhibit notable excesses. In the WWW channel, ATLAS measures 820 fb versus the SM expectation of 511 fb. The corresponding CMS result [12] is omitted due to a stringent selection cut on the azimuthal separation $\Delta\phi\left(\vec{p}_T^{3\ell}, \vec{p}_T^{\text{miss}}\right) > 2.5$, which suppresses new physics-sensitive topologies. Except for the last two WWZ measurements listed in Table 1, which fall below the SM expectation, all other measurements exhibit a clear excess over the SM predictions. These deviations are particularly intriguing in the context of the RHT model, where additional scalars can enhance triboson and top-associated production. The observed excesses thus provide an opportunity to probe and constrain such extensions of the SM.

In this proceeding, we test whether the RHT model with a 152 GeV scalar can explain these triboson anomalies. We simulate Drell–Yan production and decays of the triplet components, compute triboson cross-sections, and compare the results with LHC data to evaluate the model's viability and its implications for extended Higgs sectors.

2 Model Description: The Real Higgs Triplet Model (RHT)

We consider an extension of the SM scalar sector by a real $\text{SU}(2)_L$ Higgs triplet with zero hypercharge ($Y = 0$), commonly referred to as the RHT [16–23]. The model introduces a CP-even neutral scalar (Δ^0) and a pair of charged Higgs bosons ($\Delta^\pm$), all of which are nearly degenerate in mass due to constraints from electroweak precision measurements.

After electroweak symmetry breaking, the physical scalar spectrum consists of the SM-like Higgs boson h, identified with the 125 GeV scalar, the neutral triplet-like scalar Δ^0, and the charged scalars $\Delta^\pm$. The masses of the triplet-like scalars are approximately

$$m^2_{\Delta^0} \approx \frac{1}{2}\lambda_\Delta v^2_\Delta + \frac{A v^2_\phi}{4 v_\Delta}, \quad m^2_{\Delta^\pm} = \frac{A(v^2_\phi + 4v^2_\Delta)}{4 v_\Delta}. \tag{1}$$

where

$$\lambda_\Delta = \frac{2}{v^2_\Delta}\left(m^2_{\Delta^0} - m^2_{\Delta^\pm}\right) \tag{2}$$

and v_ϕ and v_Δ are the respective vacuum expectation values (VEVs) of the Standard Model Higgs $\text{SU}(2)_\text{L}$ doublet (Φ) with hypercharge $Y = \frac{1}{2}$ and the Higgs triplet (Δ) with $Y = 0$ respectively. The mixing angle α between the neutral scalars governs the deviation of Higgs couplings from their SM expectations and is constrained by precision Higgs measurements. The triplet vacuum expectation value v_Δ contributes at tree level only to the W boson mass.

Selection Type	ATLAS	CMS
Object Selection Criteria		
Electron	$p_T > 7$ GeV, $\|\eta\| < 2.47$	$p_T > 10$ GeV, $\|\eta\| < 2.5$
Muon	$p_T > 5$ GeV (> 15 GeV for calo-tag), $\|\eta\| < 2.7$	$p_T > 10$ GeV, $\|\eta\| < 2.4$
Jet	$p_T > 20$ GeV, $\|\eta\| < 4.5$	$p_T > 25$ GeV, $\|\eta\| < 2.4$, anti-k_T ($R = 0.4$)
b-jets	= 0	= 0
Event Preselection Criteria		
Trigger	Single-, di-, tri-, quad-lepton triggers	Same
Lepton Multiplicity	≥ 3 charged leptons	≥ 2 leptons (channel-dependent)
Z boson mass window (if applicable)	$\|m_{\ell\ell} - m_Z\| < 40$ GeV	Prompt lepton selection, tight ID/isolation
Inclusive 3ℓ Event Selection		
Preselection	✓	✓
Lepton p_T	> 15 GeV, at least one > 27 GeV	≥ 3 leptons: one > 25 GeV, others > 20 GeV (or all > 25 GeV if 0 SFOS)
SFOS dilepton mass	> 12 GeV; $\|m_{\ell\ell} - m_Z\| < 20$ GeV	> 20 GeV; $\|m_{\ell\ell} - m_Z\| > 20$ GeV for SFOS
Jet and b-jet	No b-jets; SRs based on 1 or 2 jets	No jets (1 allowed if 0 SFOS); no b-jets
Kinematic variables	—	$m_T^{\text{3rd}} > 90$ GeV, $\|\vec{p}_T^{\,3\ell}\| > 50$ GeV, $\Delta\phi > 2.5$, $\|m_{3\ell} - m_Z\| > 10$ GeV
3ℓ Signal Regions		
Region definitions	**SR1 :3**ℓ-1j : 1 jet	**3**ℓ-0SFOS
	SR2 :3ℓ-2j-inV : ≥ 2 jets, $60 < m_{jj} < 110$ GeV	**3**ℓ-1SFOS
	SR3 :3ℓ-2j-outV : ≥ 2 jets, $m_{jj} < 60$ or > 110 GeV	**3**ℓ-2SFOS
Inclusive 4ℓ Event Selection		
Preselection	✓	✓
Lepton p_T	Exactly four: 30, 15, 8, 6 GeV	Exactly four: Z pair > 25, 10 GeV; others > 25, 10 GeV
SFOS dilepton mass	> 12 GeV, $\|m_{\ell\ell} - m_Z\| < 20$ GeV	Z1: $\|m_{\ell\ell} - m_Z\| < 10$ GeV, Z2: $\|m_{\ell\ell} - m_Z\| > 10$ GeV
$\Delta R_{\ell\ell}$	> 0.1	—
E_T^{miss}	> 10 GeV	—
b-jets	= 0	= 0
4ℓ Signal Regions		
Common categories	**4**ℓ**-DF**: different-flavour W leptons ($e\mu$)	
	4ℓ**-SF-inZ**: same-flavour W leptons, $\|m_{\ell\ell} - m_Z\| < 20$ GeV	
	4ℓ**-SF-outZ**: same-flavour W leptons, $\|m_{\ell\ell} - m_Z\| > 20$ GeV	
Inclusive 5ℓ Event Selection		
Preselection	✓	✓
Leptons	≥ 5 leptons	≥ 5 leptons; leading two > 25 GeV, others > 10 GeV
Z boson candidates	≥ 2 SFOS pairs with $\|m_{\ell\ell} - m_Z\| < 20$ GeV	≥ 2 SFOS pairs with $\|m_{\ell\ell} - m_Z\| < 15$ GeV
Other cuts	—	$m_T > 50$ GeV
b-jets	= 0	= 0

Table 2: Combined summary of the object selection, event preselection, and inclusive/signal region selection criteria for 3ℓ, 4ℓ, and 5ℓ events in ATLAS and CMS analyses [11, 12].

Regarding collider phenomenology, the triplet-like scalars are primarily produced at the LHC via Drell-Yan processes,

$$q\bar{q} \to Z^*/\gamma^* \to \Delta^+\Delta^-, \qquad q\bar{q}' \to W^{\pm *} \to \Delta^0\Delta^\pm. \tag{3}$$

The neutral scalar Δ^0 predominantly decays into WW, with loop-induced channels such as $\gamma\gamma$ and $Z\gamma$ becoming relevant when the scalar is nearly degenerate with $\Delta^\pm$. The charged scalars $\Delta^\pm$ typically decay to WZ, $\tau\nu$, or tb, depending on their masses. The phenomenological implications include multilepton and diphoton final states, and the model can accommodate LHC anomalies such as excesses near 152 GeV in the diphoton spectrum. The parameter space consistent with theoretical and experimental constraints generally prefers small mixing angle α and triplet vacuum expectation values v_Δ of order 1 to 3 GeV.

3 Analysis and Results

This section covers the phenomenology related to the RHT model that was presented in earlier sections. This model helps to explain experimental results and provides guidelines for searches at certain energy and parameter choices in colliders such as the LHC.

The selection criteria summarized in Table 2 follow a tiered strategy involving lepton multiplicity, SFOS (same-flavor opposite-sign) pair counting, jet requirements, and Z-vetoes. CMS enforces tighter object-level cuts (e.g., $p_T > 10$ GeV for leptons), while ATLAS allows softer leptons to enhance sensitivity. Signal regions are defined separately in 3ℓ, 4ℓ, and 5ℓ categories, with additional kinematic requirements such as m_T, $\Delta\phi$, and E_T^{miss} cuts enhancing signal-to-background separation. Our analysis follows this structure closely, particularly employing the 3ℓ and 4ℓ categories with zero b-jet and Z-veto conditions, ensuring a consistent comparison with the reported excesses in multilepton channels.

In this study, event generation is performed using `MadGraph5_aMC@NLO` [24, 25], with parton showering via `Pythia 8.3` [26] and detector simulation using `Delphes 3.5.0` [27], configured with CMS detector parameters. Final-state objects are reconstructed from the `Delphes` output, with jets clustered using the anti-k_T algorithm (radius $R = 0.4$) via `FastJet 3.3.4` [28].

To validate the analysis framework and examine the kinematic features of the signal, we present various distributions of key observables. In particular, we examine the invariant mass distributions of same-flavour opposite-sign (SFOS) lepton pairs that are consistent with the decay of an on-shell Z boson. According to the selection criteria, each event must contain at least one SFOS lepton pair with an invariant mass within a 40 GeV window around the Z boson pole mass ($m_Z = 91.188$ GeV). Figure 1 shows the reconstructed Z boson mass from such SFOS pairs in the three signal regions (SR1, SR2, and SR3). These plots help confirm the presence of Z-boson candidates in the selected events and demonstrate the consistency of the reconstruction with the expected Z mass peak. This validation is particularly important in triboson final states such as WWZ, WZZ, tWZ, and WWW, where Z bosons are expected in the decay chain.

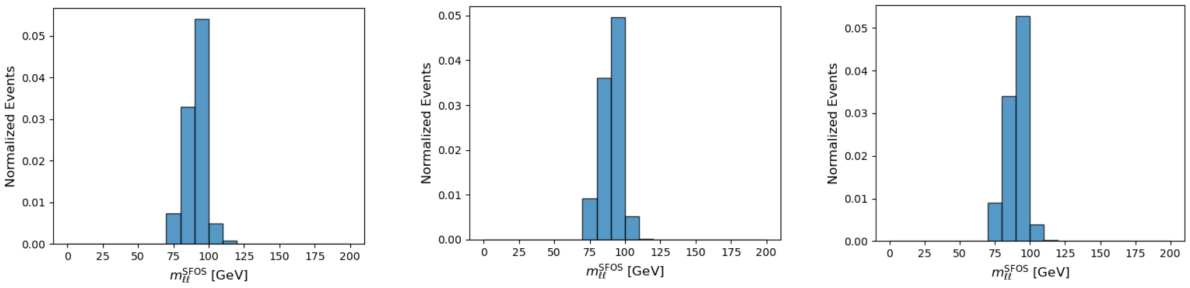

(a) SR1 (b) SR2 (c) SR3

Figure 1: Reconstructed invariant mass distributions of same-flavour opposite-sign (SFOS) lepton pairs in each signal region (SR1, SR2, and SR3).

Future Work

The next stage of the analysis involves a comprehensive treatment of relevant SM backgrounds. The production of three massive vector bosons arises from Feynman diagrams involving interaction vertices ranging from single to quartic boson couplings, as well as through the Higgsstrahlung mechanism. Additional background contributions from $t\bar{t}Z$, fake leptons, and triboson processes not involving new physics will also be modeled and validated using control regions. Following the ATLAS methodology, the signal regions will be further subdivided and optimized using multivariate techniques such as boosted decision trees, trained to enhance the separation between signal and background events. These discriminants can then be combined in a binned maximum-likelihood fit to extract a global signal strength parameter μ, defined as the ratio of the observed triboson production cross section to the Standard Model expectation. Ultimately, this strategy aims to determine whether the RHT model can quantitatively account for the observed excesses in triboson final states. Future extensions will include a global combination across channels and sensitivity projections for the upcoming Run 3 data.

References

[1] A. Crivellin, Y. Fang, O. Fischer, S. Bhattacharya, M. Kumar, E. Malwa, B. Mellado, N. Rapheeha, X. Ruan, and Q. Sha, "Accumulating evidence for the associated production of a new Higgs boson at the LHC," *Phys. Rev. D*, vol. 108, no. 11, p. 115031, 2023.

[2] S. Bhattacharya, G. Coloretti, A. Crivellin, S.-E. Dahbi, Y. Fang, M. Kumar, and B. Mellado, "Growing Excesses of New Scalars at the Electroweak Scale," 6 2023.

[3] A. M. Sirunyan *et al.*, "Measurements of Higgs boson production cross sections and couplings in the diphoton decay channel at $\sqrt{s}$ = 13 TeV," *JHEP*, vol. 07, p. 027, 2021.

[4] "Measurement of the properties of Higgs boson production at $\sqrt{s}$=13 TeV in the $H \to \gamma\gamma$ channel using 139 fb^{-1} of pp collision data with the ATLAS experiment," 8 2020.

[5] G. Aad *et al.*, "CP Properties of Higgs Boson Interactions with Top Quarks in the $t\bar{t}H$ and tH Processes Using $H \to \gamma\gamma$ with the ATLAS Detector," *Phys. Rev. Lett.*, vol. 125, no. 6, p. 061802, 2020.

[6] A. M. Sirunyan *et al.*, "Measurements of $\mathrm{t\bar{t}}H$ Production and the CP Structure of the Yukawa Interaction between the Higgs Boson and Top Quark in the Diphoton Decay Channel," *Phys. Rev. Lett.*, vol. 125, no. 6, p. 061801, 2020.

[7] G. Aad *et al.*, "Search for dark matter in events with missing transverse momentum and a Higgs boson decaying into two photons in pp collisions at $\sqrt{s}$ = 13 TeV with the ATLAS detector," *JHEP*, vol. 10, p. 013, 2021.

[8] A. M. Sirunyan *et al.*, "Search for dark matter produced in association with a Higgs boson decaying to $\gamma\gamma$ or $\tau^+\tau^-$ at $\sqrt{s} = 13$ TeV," *JHEP*, vol. 09, p. 046, 2018.

[9] A. Sirunyan *et al.*, "Search for the decay of a Higgs boson in the $\ell\ell\gamma$ channel in proton-proton collisions at $\sqrt{s} = 13$ TeV," *JHEP*, vol. 11, p. 152, 2018.

[10] G. Aad *et al.*, "Measurements of WH and ZH production in the $H \to b\bar{b}$ decay channel in pp collisions at 13 TeV with the ATLAS detector," *Eur. Phys. J. C*, vol. 81, no. 2, p. 178, 2021.

[11] Aad *et al.*, "Observation of VVZ production at $\sqrt{s} = 13$ TeV with the ATLAS detector," 12 2024.

[12] A. M. Sirunyan *et al.*, "Observation of the Production of Three Massive Gauge Bosons at $\sqrt{s}$ =13 TeV," *Phys. Rev. Lett.*, vol. 125, no. 15, p. 151802, 2020.

[13] A. Hayrapetyan *et al.*, "Measurement of WWZ and ZH production cross sections at $\sqrt{s}$ = 13 and 13.6 TeV," 5 2025.

[14] G. Aad *et al.*, "Observation of WWW Production in pp Collisions at $\sqrt{s}$ =13 TeV with the ATLAS Detector," *Phys. Rev. Lett.*, vol. 129, no. 6, p. 061803, 2022.

[15] "Observation of tWZ production at the CMS experiment," 2025.

[16] D. A. Ross and M. J. G. Veltman, "Neutral Currents in Neutrino Experiments," *Nucl. Phys. B*, vol. 95, pp. 135–147, 1975.

[17] J. F. Gunion, R. Vega, and J. Wudka, "Higgs triplets in the standard model," *Phys. Rev. D*, vol. 42, pp. 1673–1691, 1990.

[18] P. H. Chankowski, S. Pokorski, and J. Wagner, "(Non)decoupling of the Higgs triplet effects," *Eur. Phys. J. C*, vol. 50, pp. 919–933, 2007.

[19] T. Blank and W. Hollik, "Precision observables in $SU(2) \times U(1)$ models with an additional Higgs triplet," *Nucl. Phys. B*, vol. 514, pp. 113–134, 1998.

[20] J. R. Forshaw, A. Sabio Vera, and B. E. White, "Mass bounds in a model with a triplet Higgs," *JHEP*, vol. 06, p. 059, 2003.

[21] M.-C. Chen, S. Dawson, and T. Krupovnickas, "Higgs triplets and limits from precision measurements," *Phys. Rev. D*, vol. 74, p. 035001, 2006.

[22] R. S. Chivukula, N. D. Christensen, and E. H. Simmons, "Low-energy effective theory, unitarity, and non-decoupling behavior in a model with heavy Higgs-triplet fields," *Phys. Rev. D*, vol. 77, p. 035001, 2008.

[23] P. Bandyopadhyay and A. Costantini, "Obscure Higgs boson at Colliders," *Phys. Rev. D*, vol. 103, no. 1, p. 015025, 2021.

[24] J. Alwall, M. Herquet, F. Maltoni, O. Mattelaer, and T. Stelzer, "MadGraph 5 : Going Beyond," *JHEP*, vol. 06, p. 128, 2011.

[25] J. Alwall, R. Frederix, S. Frixione, V. Hirschi, F. Maltoni, O. Mattelaer, H. S. Shao, T. Stelzer, P. Torrielli, and M. Zaro, "The automated computation of tree-level and next-to-leading order differential cross sections, and their matching to parton shower simulations," *JHEP*, vol. 07, p. 079, 2014.

[26] T. Sjöstrand, S. Ask, J. R. Christiansen, R. Corke, N. Desai, P. Ilten, S. Mrenna, S. Prestel, C. O. Rasmussen, and P. Z. Skands, "An introduction to PYTHIA 8.2," *Comput. Phys. Commun.*, vol. 191, pp. 159–177, 2015.

[27] J. de Favereau, C. Delaere, P. Demin, A. Giammanco, V. Lemaître, A. Mertens, and M. Selvaggi, "DELPHES 3, A modular framework for fast simulation of a generic collider experiment," *JHEP*, vol. 02, p. 057, 2014.

[28] M. Cacciari, G. P. Salam, and G. Soyez, "FastJet User Manual," *Eur. Phys. J. C*, vol. 72, p. 1896, 2012.